

Visualization of Anode Effect in High Temperature Transparent Aluminum Electrolysis Cell

Bingliang Gao¹, Hongkun Niu², Cong Wang³ and Zhiwei Liu⁴

1. Full professor

2. Doctoral degree student

3. Doctoral degree student

4. Doctoral degree student

School of Metallurgy, Northeastern University, Shenyang, 110819, China

Corresponding author: blgao@mail.neu.edu.cn

Abstract

DOWNLOAD
FULL PAPER



The aluminum smelting industry is an important emitter of greenhouse gases. In addition to the emission of CO₂ during normal operation, perfluorocarbons (PFCs) are generated when the Al₂O₃ concentration in the electrolyte falls below a certain critical level – a phenomenon referred to as *anode effect*. It is important that the mechanism of anode effect formation is well-understood to devise means of mitigating its occurrence. In this paper, the anode effect occurring at an industrial grade carbon anode with an underside surface area of 50 cm² (10 cm × 5 cm) was observed in a high temperature transparent electrolytic cell operating at 940 °C. The visual observation of the phenomenon confirmed that the anode effect is caused by the formation of an intermediate, insulating CF_x film. No gas layer or large bubbles were observed during the anode effect. The sharp increase of the cell voltage is caused by the insulating nature of the intermediate continuous unbroken film formed on the anode.

Keywords: Aluminum electrolysis, Transparent aluminum electrolysis cell, Carbon anode, Anode effect, PFC emissions.

1. Introduction

Hall-Héroult process is the only industrial process for primary aluminum production since 1886. Under normal electrolysis conditions, CO₂ is mainly released from the carbon anode. Under perturbed conditions when the alumina concentration falls below a critical level, perfluorocarbons (PFCs) consisting mostly of CF₄ with small amounts of C₂F₆ are generated on the carbon anode, accompanied by a cell voltage rise from about 4 V to about 20–65 V within a short time. The phenomenon is referred to as anode effect (AE) [1-2].

PFCs are potent greenhouse gases (GHGs) with extremely long lifetimes in the atmosphere and with high global warming potentials (GWPs). For example, CF₄ has a lifetime of 50 000 years and GWPs at 6 500 times the equivalent of CO₂ [3].

Most interpretations of the anode effect available in the literature may be summarized as combination of three causes [2, 4-10]:

- 1) Excessive increase in the concentration overpotential caused by depletion of dissolved alumina (Al₂O₃) near the interface of the anode/electrolyte;
- 2) The formation of intermediate carbon fluoride (CF_x) on the anode because of discharge of fluorine-containing ions;
- 3) The formation of a blanketing layer of a gaseous phase underneath the anode caused by a change in wettability of the anode to the electrolyte, which blocks the anodic current flow path to the electrolyte, resulting in a sharp increase of cell voltage.

In this paper, a see-through electrolytic cell operating at 940 °C was used to observe the anode effect occurring on an industrial grade carbon anode in a molten solution of Na₃AlF₆-AlF₃-LiF-CaF₂-Al₂O₃.

2. Experimental

Electrolyte (molar ratio of NaF/AlF₃ = 2.2) used in the experiment was a mixture of NaF (45.6 wt%), AlF₃ (41.4 wt%), CaF₂ (5 wt%), Al₂O₃ (3 wt%), LiF (5 wt%), which has a liquidus temperature of 920.9 °C. All chemicals were dried at 400 °C for more than 4 hours before use. The total weight of electrolyte used during the electrolysis experiments was 0.5 kg. Industrial anode material was used during the electrolysis experiments. The graphite cathodes were fabricated using high-purity graphite (Purity 99 %) by Kejin Graphite Ltd, Shenyang China. The industrial grade carbon anode was sampled from an aluminum smelter in China.

A high temperature see-through electrolysis cell was used for studying the phenomenon of anode effect occurring in the cryolite-based melt. The specific experimental details can be found in reference [11]. Here, a brief description of the experimental details will be provided. A high temperature see-through electrolysis cell, as shown in Figure 1, consists of a three-chamber quartz crucible with a middle chamber as the anodic compartment and two side chambers as the cathodic compartments (5). The entire crucible is held inside an electric furnace (3) with a bottom-observation window (7) and a side-observation window (10). There is also provided an image recording system (9), a data collecting system (8), and a 200 A DC power supply (1). There is a gap (2 mm high) between the quartz separating wall and bottom of the crucible, acted as a tunnel for bath flow and DC current flow between chambers. The carbon anode measures 100×50×70 mm, with the underside working surface area of 50 cm². Two graphite cathodes, each measures 50×12×70 mm, provide a total underside surface area of 12 cm². The current density of anode (ACD) applied was in the range of 0.3-1.5 A/cm² with intervals of 0.6 A/cm². Industrial carbon anode was electrolyzed for about 20 minutes at different current densities.

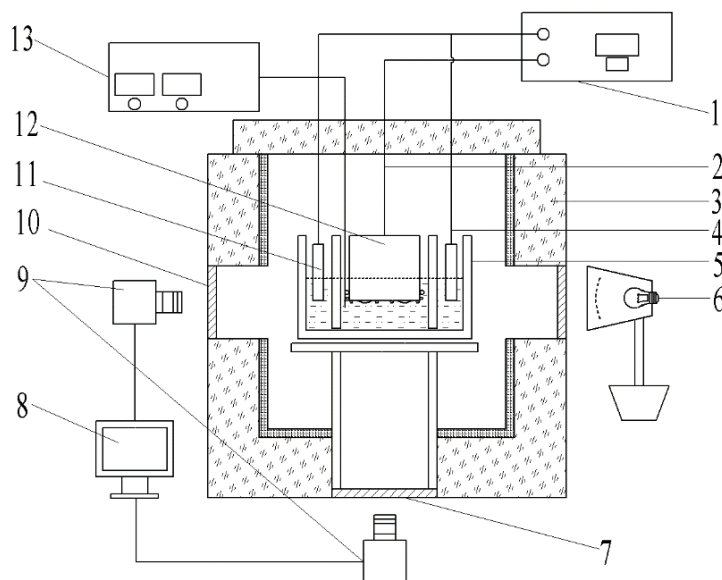


Figure1. Schematic diagram of the high temperature see-through aluminum electrolytic cell set-up.

1- 200 A DC power supply; 2- Anode current collecting rod; 3- Electric furnace; 4- Cathode current collecting rod; 5- Three-chamber quartz crucible; 6- Light source; 7- Bottom-observation quartz window; 8- Computer; 9- High speed camera; 10- Side-observation quartz window; 11- Graphite cathode; 12- Carbon anode; 13- Temperature controller.

4. Conclusion

In this work, a see-through high temperature cell was used to study the bubble behavior at an industrial carbon anode at anodic current densities ranging from 0.3 to 1.5 A/cm². The phenomenon of anode effect at an industrial carbon anode was observed when the current density of anode was 1.5 A/cm².

During the anode effect, no bubbles or persistent bubble layer blanketing the anode bottom surface was observed. We did observe the growth of a bubble-free area accompanied by a 'fire-ball' type of explosion and a loud noise. The exfoliated films during the anode effect were observed and considered as CF_x with value of x greater than 0.25 based on its density evaluation. CF_x has very high resistivity and contributes to the sharp rise of the cell voltage. Due to the insulation of the CF_x film at the fluorinated area, it will cease both the oxidation of oxygen ions and bubble formation. Therefore, bubble-free area starts growing and expands eventually. Hence, working area of the anode decreases, which promotes fluorination of carbon atoms and initiates anode effect. It confirms that the anode effect is caused by the formation of intermediate insulating CF_x film.

5. References

1. Alton T. Tabereaux, Anode effects, PFCs, global warming, and the aluminum industry, *JOM*, 1994, 46(11), 30-34.
2. Warren Haupin and Edward J. Seger, Aiming for zero anode effects, *Light Metals* 2001, 767-773.
3. Eric Jay Dolin, PFC emissions reductions: the domestic and international perspective, *Light Metal Age-CHICAGO-*, 1999, 57, 56-67.
4. David S. Wong et al., PFC emissions from detected versus nondetected anode effects in the aluminum industry, *JOM*, 2015, 67, 342-353.
5. J. Thonstad, F. Nordmo and K. Vee, On the anode effect in cryolite-alumina melts-I, *Electrochimica Acta*, 1973, 18(1), 27-32.
6. J. Thonstad, F. Nordmo and J. K. Rødseth, On the anode effect in cryolite-alumina melts-II the initiation of the anode effect, *Electrochimica Acta*, 1974, 19(11), 761-769.
7. H. Vogt, On the mechanism of the anode effect in aluminum electrolysis, *Metallurgical and Materials Transactions B*, 2000, 31, 1225-1230.
8. H. Vogt, On the various types of uncontrolled potential increase in electrochemical reactors-The anode effect, *Electrochimica acta*, 2013, 87, 611-618.
9. H. Vogt, The anode effect as a fluid dynamic problem, *Journal of applied electrochemistry*, 1999, 29, 137-145.
10. Zhu-xian Qiu and Ming-jie Zhang, Studies on anode effect in molten salts electrolysis, *Electrochimica acta*, 1987, 32(4), 607-613.
11. Bing-liang Gao et al., Visualization of Anode Effect in Aluminum Electrolysis, *Journal of The Electrochemical Society*, 2022, 169(1), 013505.
12. Warren Haupin, Interpreting the components of cell voltage, *Light Metals* 2016, 153-159.
13. Zhi-bin Zhao et al., Observation of anodic bubble behaviors using laboratory scale transparent aluminium electrolysis cells, *Light Metals* 2015, 801-806.
14. Zhi-bin Zhao et al., Anodic bubble behavior and voltage drop in a laboratory transparent aluminium electrolytic cell, *Metallurgical and materials Transactions B*, 2016, 47, 1962-1975.
15. Matthew H. Luly, Electrical resistivity of fluorinated carbon black, *Journal of Materials Research*, 1988, 3(5), 890-897.
16. Halvor Kvande, The structure of alumina dissolved in cryolite melts, *Light Metals* 1986, 96-104.

17. Gong Chen et al., Electrochemical behavior of graphite anode during anode effect in cryolite molten salts, *Transactions of Nonferrous Metals Society of China*, 2012, 22(9), 2306-2311.
18. A.K. Kuriakose and J.L. Margrave, Kinetics of the reactions of elemental fluorine. IV. Fluorination of graphite, *The Journal of Physical Chemistry*, 1965, 69(8), 2772-2775.